https://doi.org/10.3311/PPci.20123

Periodica Polytechnica Civil Engineering, 66(4), pp. 1207–1219, 2022

An Iterative Two-step Lagrangian-based Method for Evaluation of Structural Reliability Index

Mohammad Amin Roudak[1*], Mohammad Karamloo[2], Mohsen Ali Shayanfar[3]

[1] Department of Civil Engineering, Faculty of Engineering, Alzahra University, Vanak St., 1993893973 Tehran, Iran
[2] Department of Civil Engineering, Shahid Rajaee Teacher Training University, Lavizan, 1678815811 Tehran, Iran
[3] School of Civil Engineering, Centre of Excellence for Fundamental Studies in Structural Engineering, Iran University of Science and Technology, Hengam St., 1311416846 Tehran, Iran
[*] Corresponding author, e-mail: a.roudak@alzahra.ac.ir

Received: 07 March 2022, Accepted: 18 August 2022, Published online: 01 September 2022

Abstract

In structural reliability analysis, Hasofer-Lind and Rackwitz-Fiessler (HL-RF) method is a widely used approximation method for evaluating the reliability index. However, by increasing the nonlinearity or complexity in the limit state function of a structure, HL-RF may get in trouble for convergence. This paper represents an iterative algorithm that tries to minimize the Lagrange function, associated with the reliability problem. In each iteration of this method, two steps are followed, to satisfy the minimization condition and the existing constraint. In the first step, a movement for minimization in a descent direction is followed. In the second step, another search direction contributes to approach limit state surface, and therefore the next iteration can start from the vicinity of the surface. Employing Lagrange reliability function and limit state function simultaneously in the proposed two-step Lagrangian-based method (TSLB) can help to control the numerical instability in highly nonlinear problems. The accuracy and robustness of the proposed algorithm are shown in illustrative examples of the literature.

Keywords

two-step Lagrangian-based method (TSLB), reliability index, limit state function, HL-RF method

1 Introduction

Structural reliability analysis deals with the issue of uncertainty in structural problems [1–3]. In a structure, uncertainty can be observed in materials, loads and geometry. Evaluation of the probability of failure in the presence of uncertainty is the main purpose in structural reliability analysis [4–6]. The following definite multi-dimensional integral gives the probability of failure

$$P_f = \int_{g(\boldsymbol{X})<0} f_{\boldsymbol{X}}(\boldsymbol{X}) d\boldsymbol{X} \,, \tag{1}$$

where the vector $\boldsymbol{X} = [X_1, X_2,\ldots,X_n]^T$ represents n random variables. $f_{\boldsymbol{X}}(\boldsymbol{X})$ is the joint probability density function (JPDF) of the vector $\boldsymbol{X}$. $g(\boldsymbol{X})$ is limit state function (LSF) and $g(\boldsymbol{X}) < 0$ defines failure domain. Direct evaluation of the integral of Eq. (1) will be extremely challenging if the problem is complex. Simulation methods such as Monte Carlo simulation (MCS) [7–9], or approximation methods [10–12] are brought up as the alternatives. The exact solution is accessible in MCS, but at the cost of generating too many samples. Besides, MCS may not be reliable when the probability of failure is too small [13]. Among approximation methods, first-order reliability method (FORM) has been greatly developed for practice. In 1969, Cornell [14] proposed to linearize about the mean value of LSF. Reliability index in his method is the proportion of the mean to standard deviation of LSF. This method depends on the mathematical formulation of the problem and actually fails to be invariant. Hasofer and Lind [15] proposed to linearize about the so-called design point or most probable point (MPP). This point lies in the limit state surface and has the minimum distance from the origin of the standard normal coordinate system. Hasofer and Lind defined this minimum distance reliability index. Rackwitz and Fiessler [16] extended the Hasofer-Lind method to consider the distribution of random variables. The Hasofer-Lind method modified by Rackwitz and Fiessler, is denoted by HL-RF. For many situations, this method converges very fast. However, in highly nonlinear LSFs, the method may

Cite this article as: Roudak, M. A., Karamloo, M., Shayanfar, M. A. "An Iterative Two-step Lagrangian-based Method for Evaluation of Structural Reliability Index", Periodica Polytechnica Civil Engineering, 66(4), pp. 1207–1219, 2022. https://doi.org/10.3311/PPci.20123

result in divergence. Liu and Der Kiureghian [17] modified HL-RF by introducing a merit function to monitor the convergence. Wang and Grandhi [18] improved HL-RF using intervening variables. Santosh et al. [19] applied an efficient step length selection rule in iterations. Yang et al. [20] and Yang [21] used chaos theory and represented stability transformation method (STM). Gong and Yi [22] introduced a step size parameter in the direction of gradient vector of limit state function. As the step size goes extremely large the method reduces to HL-RF. Keshtegar and Miri [23] proposed relaxed HL-RF (RHL-RF) by applying a relaxed coefficient and second-order fitting of the reliability function. Gong et al. [24] proposed a non-gradient-based algorithm in reliability analysis. Roudak et al. [25] proposed a robust two-parameter method as the generalization of HL-RF. Specific values for each of these two parameters, reduce the method to HL-RF. When only the first parameter takes a specific value, the method reduces to the method proposed by Gong and Yi. In another study, Roudak et al. [26] proposed a three-phase algorithm by introduction of a moving fitness function. Combining the concepts of approximation methods and sampling of simulation methods, Shayanfar et al. [27, 28] represented two methods of searching design point. Shayanfar et al. [29] included a new transformation in HL-RF to deal with skew-distributed random variables. Roudak and Karamloo [30] established the non-negative constraint method as an improvement in the category of first-order reliability methods.

In this paper, an algorithm is proposed to compute reliability index. This algorithm minimizes the Lagrange function of reliability problems iteratively and using two steps. This two-step Lagrangian-based method (TSLB) is implemented in mathematical and structural problems. The represented search direction vectors and step sizes have made the proposed algorithm robust and relatively efficient.

2 HL-RF method

The main purpose in HL-RF method is to minimize the distance of LSF from the origin of standard normal coordinate system or *U*-space. This minimum distance, denoted by β, is reliability index. Thus, the calculation of the reliability index can be formulated as the following constrained optimization problem

$$\begin{cases} \beta = \min(\boldsymbol{U}^T\boldsymbol{U})^{1/2} \\ \text{subject to: } G(\boldsymbol{U}) = 0 \end{cases}, \tag{2}$$

where $G(\boldsymbol{U})$ is LSF in *U*-space. Random variables in HL-RF, according to the suggestion of Rackwitz and Fiessler [16], are transformed from the original *X*-space to the transformed *U*-space by the following transformation

$$U_i = \frac{X_i - \mu'_{X_i}}{\sigma'_{X_i}}, \tag{3}$$

where μ'_{Xi} and σ'_{Xi} are called mean and standard deviation of the equivalent normal distribution, respectively. These are calculated by

$$\sigma'_{X_i} = \frac{\phi\left\{\Phi^{-1}\left[F_{X_i}(x_i^*)\right]\right\}}{f_{X_i}(x_i^*)}, \tag{4}$$

$$\mu'_{X_i} = -\sigma'_{X_i}\Phi^{-1}\left[F_{X_i}(x_i^*)\right] + x_i^*. \tag{5}$$

ϕ and Φ are the probability density function (PDF) and cumulative distribution function (CDF) of standard normal distribution, respectively. Design point in HL-RF method can be computed by the following recursive formula

$$\boldsymbol{U}_{k+1} = \frac{\nabla^T G(\boldsymbol{U}_k)\boldsymbol{U}_k - G(\boldsymbol{U}_k)}{\nabla^T G(\boldsymbol{U}_k)\nabla G(\boldsymbol{U}_k)}\nabla G(\boldsymbol{U}_k), \tag{6}$$

where $\boldsymbol{U}_k$ and $\boldsymbol{U}_{k+1}$ are design points at iteration k and $k + 1$, respectively.

3 Proposed algorithm

In this section, an iterative algorithm for finding design point is to be proposed. To do so, suppose design point of iteration k ($\boldsymbol{U}_k$) is known and the next design point at iteration $k + 1$ ($\boldsymbol{U}_{k+1}$) is to be found. At the first step of each iteration, $\boldsymbol{U}_k$ is moved on a descent direction to reach $\boldsymbol{U}'_k$. Since this point is not necessarily located on limit state surface, at the second step, it is moved on another vector such that it approaches limit state surface. A design point on limit state surface provides a more appropriate seedbed for the next iterations [17]. The point that is now closer to limit state surface, is new design point of iteration $k + 1$, denoted by $\boldsymbol{U}_{k+1}$. Two movements from $\boldsymbol{U}_k$ to $\boldsymbol{U}'_k$ and from $\boldsymbol{U}'_k$ to $\boldsymbol{U}_{k+1}$ can be seen in Fig. 1. Two step sizes α_k and γ_k and two search direction vectors $\boldsymbol{d}_k$ and $\boldsymbol{S}_k$, illustrated in the figure, will be introduced in the following.

For starting the formulation of the proposed Two-Step Lagrangian-Based method (TSLB), consider the Lagrange or reliability function

$$f(\boldsymbol{U}) = \frac{1}{2}\boldsymbol{U}^T\boldsymbol{U} + \lambda G(\boldsymbol{U}), \tag{7}$$

associated with the reliability problem of Eq. (2). Design point is the point minimizing this function. For a local minimum point, the following equations should be satisfied

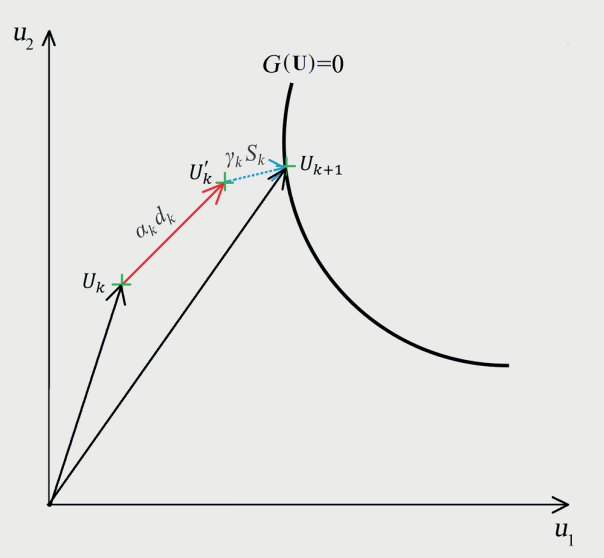

Fig. 1 General two-step movement of the proposed algorithm

$$\boldsymbol{U}+\lambda\nabla G(\boldsymbol{U})=0\,, \tag{8}$$

$$G(\boldsymbol{U})=0\,, \tag{9}$$

where λ is Lagrange multiplier. Equation (8) results in the following relation for λ at iteration k [17, 23]

$$\lambda_k=-\frac{\nabla^T G(\boldsymbol{U}_k)\boldsymbol{U}_k}{\nabla^T G(\boldsymbol{U}_k)\nabla G(\boldsymbol{U}_k)}\,. \tag{10}$$

On the other hand, in order to satisfy both conditions of the constrained minimization problem two movements are followed in each iteration, one to minimize the value of the objective function f, and the other to satisfy the constraint $G = 0$. The movement of the first step from $\boldsymbol{U}_k$, results in $\boldsymbol{U}'_k$ as

$$\boldsymbol{U}'_k=\boldsymbol{U}_k+\alpha_k\boldsymbol{d}_k\,, \tag{11}$$

where the scalar α_k and the vector $\boldsymbol{d}_k$ are step size and search direction vector, respectively. For minimizing the function f of Eq. (7), $\boldsymbol{d}_k$ should be a descent direction. In fact, at this step, the purpose is just to move on such a descent direction, and then the resulted point will be modified at the next step.

Among many possible descent directions, opposite of the gradient vector of f at $\boldsymbol{U}_k$, i.e., $-\nabla f(\boldsymbol{U}_k)$, is selected, of course after dividing by its magnitude to make it a unit vector. Thus, $\boldsymbol{d}_k$ to be used in Eq. (11) is

$$\boldsymbol{d}_k=-\frac{\nabla f(\boldsymbol{U}_k)}{\left\|\nabla f(\boldsymbol{U}_k)\right\|}\,, \tag{12}$$

where $\nabla f(\boldsymbol{U}_k)$, according to Eq. (7), is

$$\nabla f(\boldsymbol{U}_k)=\boldsymbol{U}_k+\lambda_k\nabla G(\boldsymbol{U}_k)\,, \tag{13}$$

in which λ_k is replaced from Eq. (10). It is noted that the coefficient λ_k is not to be chosen arbitrarily. In fact, Lagrange multiplier λ_k is required to designate Lagrange function of Eq. (7), and this is carried out by λ_k taking the specific value presented in Eq. (10). This step of the proposed algorithm is completed by selecting a value for the coefficient α_k as step size of the movement. Since the movement is on a descent direction, any relatively small value for α_k can be used for this proposed algorithm. However, this value needs to be smaller for nonlinear LSFs. Our suggestion is to start with a specific value and reduce it in iterations if necessary, although a fixed value is also possible. To do so, the initial value is selected to be 0.5 and it will be divided by a constant (e.g., 1.5) if the value of f increases in iterations, instead of decreasing. Thus

$$\alpha_k=\begin{cases}0.5 & k=1\\ \alpha_{k-1} & f_k\le f_{k-1}\\ \alpha_{k-1}/1.5 & f_k>f_{k-1}\end{cases}\,. \tag{14}$$

After moving on the descent direction $\boldsymbol{d}_k$ and determination of $\boldsymbol{U}'_k$, the second step starts. At this step, $\boldsymbol{U}_{k+1}$ is obtained by transferring $\boldsymbol{U}'_k$ to limit state surface. This transferring at each iteration helps to satisfy Eq. (9) and provides a better seedbed for movement at the proceeding iteration. Suppose $\boldsymbol{U}_{k+1}$ and $\boldsymbol{U}'_k$ are related by

$$\boldsymbol{U}_{k+1}=\boldsymbol{U}'_k+\gamma_k\boldsymbol{S}_k\,, \tag{15}$$

where $\boldsymbol{S}_k$ is a vector on which the value of G is to change. Thus, $\boldsymbol{S}_k$ is selected to be

$$\boldsymbol{S}_k=-\frac{\nabla G(\boldsymbol{U}'_k)}{\left\|\nabla G(\boldsymbol{U}'_k)\right\|}\,. \tag{16}$$

The scalar γ_k in Eq. (15) is computed such that the condition of Eq. (9) is satisfied. Since G can be generally a complicated nonlinear function, the first-order approximation of Taylor expansion around $\boldsymbol{U}'_k$ is used instead of the original G. Thus, setting this approximation to zero, to satisfy Eq. (9), results in

$$G(\boldsymbol{U}_{k+1})\approx G(\boldsymbol{U}'_k)+\nabla^T G(\boldsymbol{U}'_k)(\boldsymbol{U}_{k+1}-\boldsymbol{U}'_k)=0\,. \tag{17}$$

Equation (15) is placed in the above equation to reach

$$G(\boldsymbol{U}'_k)+\gamma_k\nabla^T G(\boldsymbol{U}'_k)\boldsymbol{S}_k=0\,, \tag{18}$$

and therefore γ_k is computed as

$$\gamma_k=-\frac{G(\boldsymbol{U}'_k)}{\nabla^T G(\boldsymbol{U}'_k)\boldsymbol{S}_k}\,. \tag{19}$$

Now $\boldsymbol{U}_{k+1}$ of Eq. (15) can be found. Consequently, reliability index of iteration $k+1$ is computed by

$$\beta_{k+1} = \|\boldsymbol{U}_{k+1}\|. \tag{20}$$

The applied points ($\boldsymbol{U}_k$, $\boldsymbol{U}'_k$ and $\boldsymbol{U}_{k+1}$), step sizes (α_k and γ_k), search direction vectors ($\boldsymbol{d}_k$ and $\boldsymbol{S}_k$), alongside the direction of each vector (i.e., $-\nabla f(\boldsymbol{U}_k)$ and $-\nabla G(\boldsymbol{U}'_k)$) are summarized in Fig. 2. It will be shown in numerical examples that making use of the gradient of both functions f and G can effectively work.

To sum up briefly, the present paper proposes an iterative formulation to find $\boldsymbol{U}_{k+1}$ from $\boldsymbol{U}_k$. First, $\boldsymbol{U}'_k$ is computed by Eq. (11). The constituents of this equation are computed by Eqs. (12)–(14). Then, Eq. (15) is used to compute $\boldsymbol{U}_{k+1}$, the constituents of which are computed by Eqs. (16) and (19). To clarify the implementation of TSLB in reliability problems, flowchart of TSLB is provided in Fig. 3, showing that the steps are very simple. However, according to the results of the following numerical examples, these simple steps can effectively work.

4 Results and discussion

Several numerical examples have been brought herein from the literature, to show the behavior of the proposed algorithm. In each example, iteration history of TSLB is compared with HL-RF, Relaxed HL-RF (RHL-RF) and stability transformation method (STM). Moreover, a table is provided to compare the final values of these methods. In the following, nine reliability examples are presented and after that, they will be analyzed by reliability methods including the proposed TSLB.

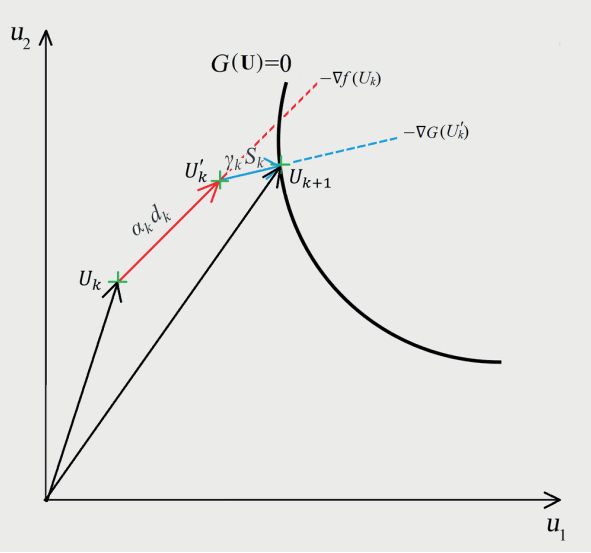

Fig. 2 Direction of movements using reliability function f and LSF G

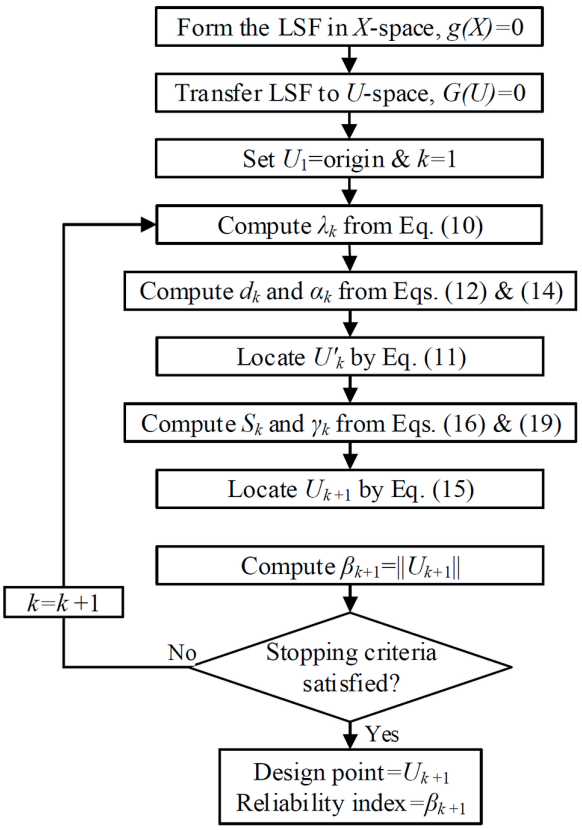

Fig. 3 Flowchart of TSLB

Example 1. The following cubic polynomial is considered the LSF of this example

$$g(x) = x_1^3 + x_2^3 - 18, \tag{21}$$

where x_1 and x_2 have normal distribution with means $\mu_1 = 10$, $\mu_2 = 9.9$ and standard deviations $\sigma_1 = \sigma_2 = 5$.

Example 2. Keeping the same statistics as the previous example, in this example a mixed term is added to the LSF

$$g(x) = x_1^3 + x_1^2 x_2 + x_2^3 - 18. \tag{22}$$

Example 3. The quartic LSF in this example is defined

$$g(x) = x_1^4 + 2x_2^4 - 20, \tag{23}$$

where x_1 and x_2 have normal distribution with means $\mu_1 = \mu_2 = 10$ and standard deviations $\sigma_1 = \sigma_2 = 5$.

Example 4. This example investigates the polynomial

$$g(x) = x_1^3 + x_2^3 - 67.5, \tag{24}$$

where x_1 and x_2 have normal distribution with means $\mu_1 = 10$, $\mu_2 = 9.9$ and standard deviations $\sigma_1 = \sigma_2 = 5$.

Example 5. A cosine function is added to a polynomial as

$$g(x) = -0.16(x_1 - 1)^3 - x_2 + 4 - 0.04\cos(x_1 x_2), \tag{25}$$

with x_1 and x_2 as standard normal variables.

Example 6. A highly nonlinear LSF with six lognormal variables is to be investigated in this example. This LSF is composed of linear terms and noise terms as follows

$$g(x) = x_1 + 2x_2 + 2x_3 + x_4 - 5x_5 - 5x_6 + 0.001\sum_{i=1}^{6}\sin(100x_i). \quad (26)$$

The statistics of the random variables are listed in Table 1.

Example 7. As a severe test for the proposed algorithm, a highly nonlinear LSF corresponding to the 2-degree-of-freedom primary-secondary system of Fig. 4 is studied. The random variables of this problem are the masses m_p and m_s, stiffnesses k_p and k_s, damping ratios ζ_p and ζ_s, the force capacity of the secondary spring F_s, and the intensity of a white-noise base excitation of the system S_0. The subscripts p and s denote the primary and secondary oscillators, respectively. The statistics of these random variables are summarized in Table 2.

Table 1 Statistics of random variables in Example 6

Variable	Distribution	Mean	Standard deviation
x_1	Lognormal	120	12
x_2	Lognormal	120	12
x_3	Lognormal	120	12
x_4	Lognormal	120	12
x_5	Lognormal	50	15
x_6	Lognormal	40	12

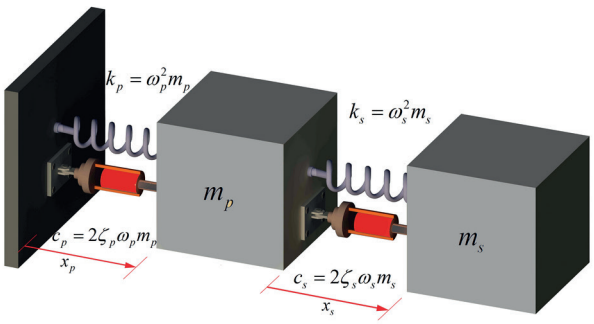

Fig. 4 Primary-secondary dynamic system of Example 7 [30]

Table 2 Statistics of random variables in Example 7

Variable	Distribution	Mean	Standard deviation
m_p	Lognormal	1	0.1
m_s	Lognormal	0.01	0.001
k_p	Lognormal	1	0.2
k_s	Lognormal	0.01	0.002
ζ_p	Lognormal	0.05	0.02
ζ_s	Lognormal	0.02	0.01
F_s	Lognormal	15	1.5
S_0	Lognormal	100	10

The LSF of this dynamic system is expressed by

$$g = F_s - k_s p\sqrt{E}\,, \quad (27)$$

$$E = \frac{\pi S_0}{4\zeta_s\omega_s^3}\left[\frac{\zeta_a\zeta_s}{\zeta_p\zeta_s(4\zeta_a^2+\eta^2)+\upsilon\zeta_a^2}\frac{(\zeta_p\omega_p^3+\zeta_s\omega_s^3)\omega_p}{4\zeta_a\omega_a^4}\right], \quad (28)$$

with $\omega_p = (k_p/m_p)0.5$, $\omega_s = (k_s/m_s)0.5$, $\omega_a = (\omega_p + \omega_s)/2$, $\zeta_a = (\zeta_p + \zeta_s)/2$, $\upsilon = m_s/m_p$, $\eta = (\omega_p - \omega_s)/\omega_a$ and $p = 3$.

Example 8. Consider the column of Fig. 5 with length L, modulus of elasticity E and moment of inertia I, under the loads H and P. This column is connected to the base by a rotational spring with constant b. The LSF is defined

$$g = 10 - \Delta\,, \quad (29)$$

$$\Delta = \frac{H}{EI\left(P/EI\right)^{\frac{3}{2}}}\times\left[\tan\left(L\sqrt{P/EI}\right) - L\sqrt{P/EI} + \frac{b^2\left\{1-\sqrt{1-\frac{4HEI}{b^2}\tan^2\left(L\sqrt{P/EI}\right)}\right\}^2}{4HEI\tan\left(L\sqrt{P/EI}\right)}\right]. \quad (30)$$

The characteristics of random variables are provided in Table 3.

Example 9. The cantilever tube of Fig. 6 is subjected to three forces F_1, F_2 and P, and one torsion T.

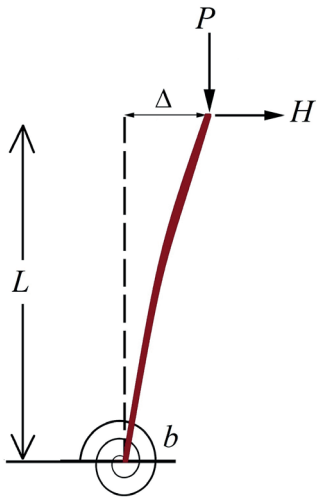

Fig. 5 Column of example 8 [30]

Table 3 Statistics of random variables in Example 8

Variable	Distribution	Mean	Standard deviation
P (kips)	Lognormal	10	3
H (kips)	Lognormal	5.8	1.16
E (ksi)	Lognormal	2.9×10^4	0.58×10^4
L (in)	Lognormal	144	7.2
I (in4)	Lognormal	88.6	8.86
b (in.kips/rad)	Lognormal	3×10^4	0.3×10^4

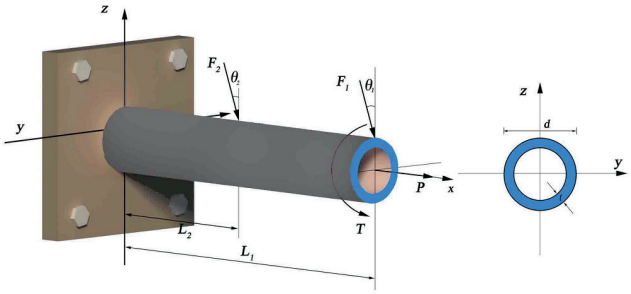

Fig. 6 Cantilever tube of Example 9 [30]

The LSF of this example is defined as

$$g = S_y - \sqrt{\sigma_x^2 + 3\tau_{zx}^2}\,, \tag{31}$$

in which S_y is the strength. σ_x and τ_{zx} are given by

$$\sigma_x = \frac{P + F_1 \sin\theta_1 + F_2 \sin\theta_2}{A} + \frac{Md}{2I}, \quad \tau_{zx} = \frac{Td}{4I}, \tag{32}$$

where

$$\begin{cases} M = F_1 L_1 \cos\theta_1 + F_2 L_2 \cos\theta_2 \\ A = \dfrac{\pi}{4}\left[d^2 - (d-2t)^2\right] \\ I = \dfrac{\pi}{64}\left[d^4 - (d-2t)^4\right] \end{cases}. \tag{33}$$

The characteristics of the variables are summarized in Table 4.

In this part, the above-mentioned examples are to be investigated. For 2-dimensional examples, i.e., examples 1 to 5, the LSFs have been drawn to reflect the characteristics of the functions schematically (Figs. 7–11).

Figs. 12–20 illustrate the performance of TSLB, HL-RF, RHL-RF and STM in the above examples. Besides, the answers for reliability indices and the number of iterations

Table 4 Statistics of random variables in Example 9

Variable	Distribution	Mean	Standard deviation
t (mm)	Normal	5	0.1
d (mm)	Normal	42	0.5
L_1 (mm)	Normal	119.75	11.975
L_2 (mm)	Normal	59.75	5.975
F_1 (N)	Lognormal	3000	300
F_2 (N)	Lognormal	3000	300
P (N)	Lognormal	12000	1200
T (N.mm)	Gumbel	90000	9000
S_y (MPa)	Normal	220	22
θ_1 (rad)	Normal	0	π/4
θ_2 (rad)	Normal	0	π/4

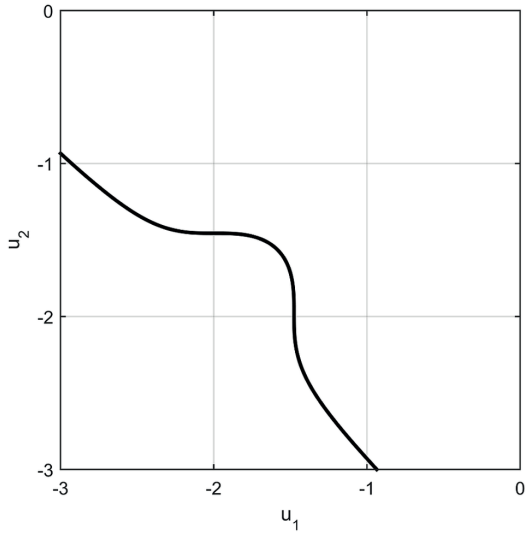

Fig. 7 Limit state function of example 1 in U-space

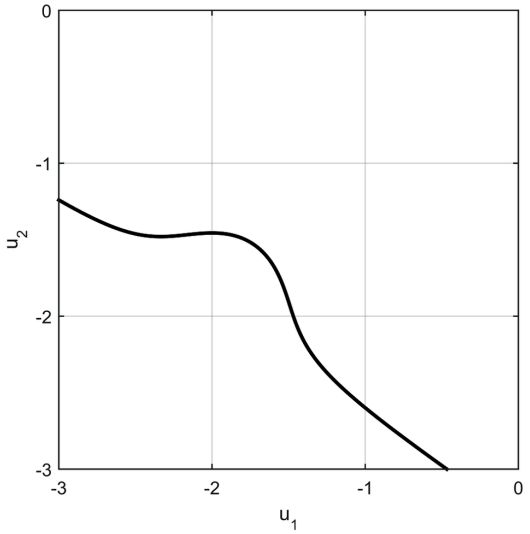

Fig. 8 Limit state function of example 2 in U-space

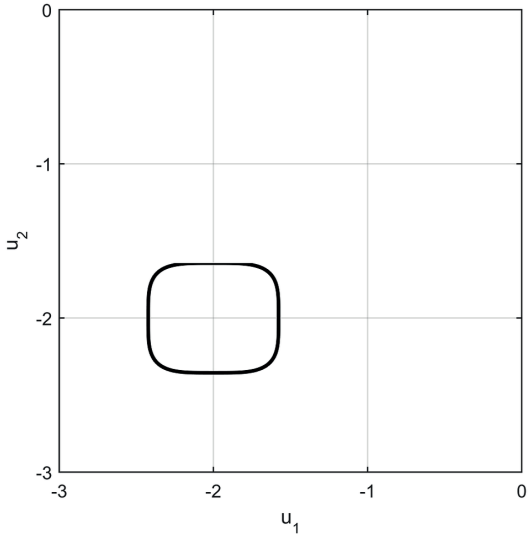

Fig. 9 Limit state function of example 3 in U-space

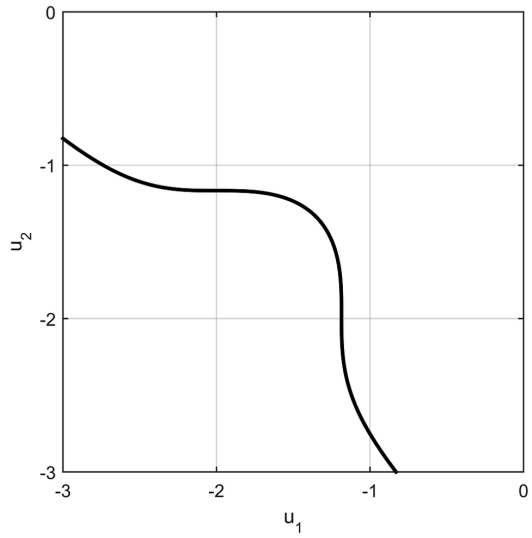

Fig. 10 Limit state function of example 4 in U-space

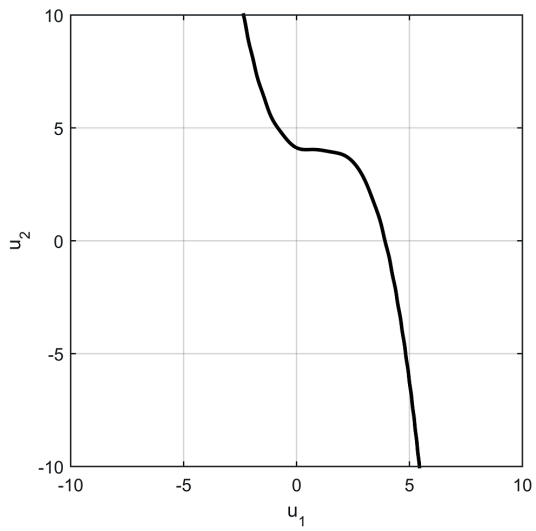

Fig. 11 Limit state function of example 5 in U-space

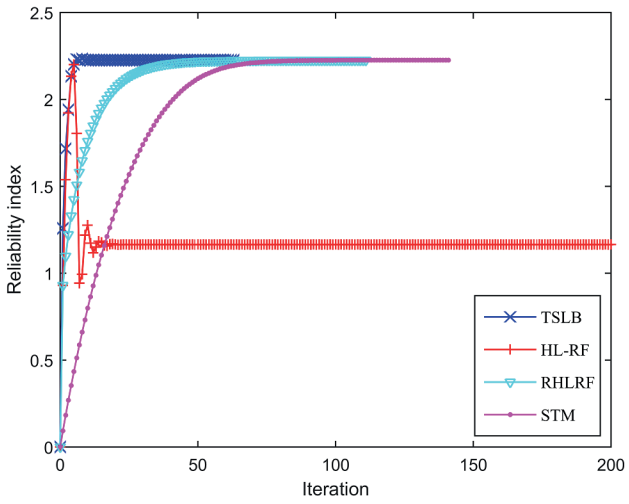

Fig. 12 Iteration history in example 1

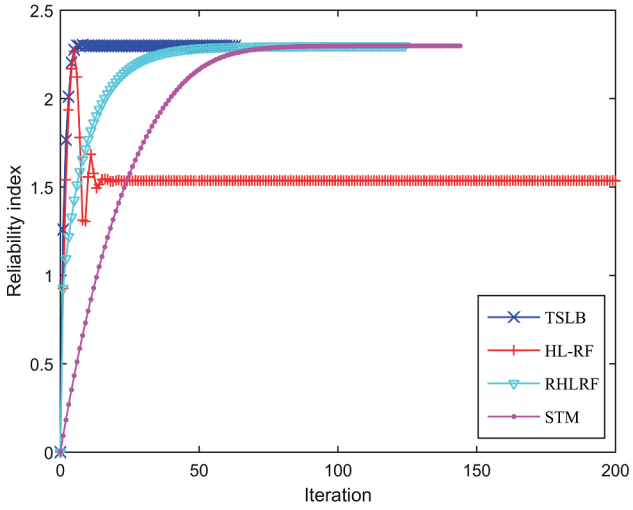

Fig. 13 Iteration history in example 2

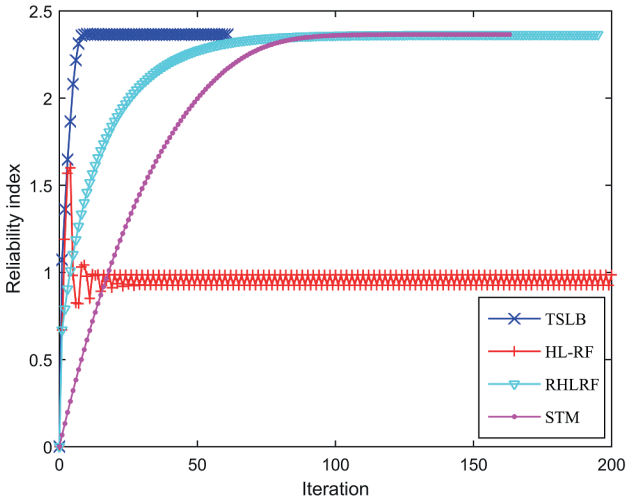

Fig. 14 Iteration history in example 3

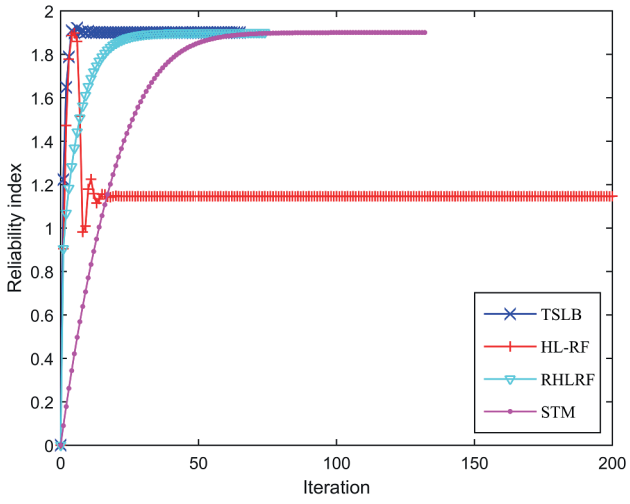

Fig. 15 Iteration history in example 4

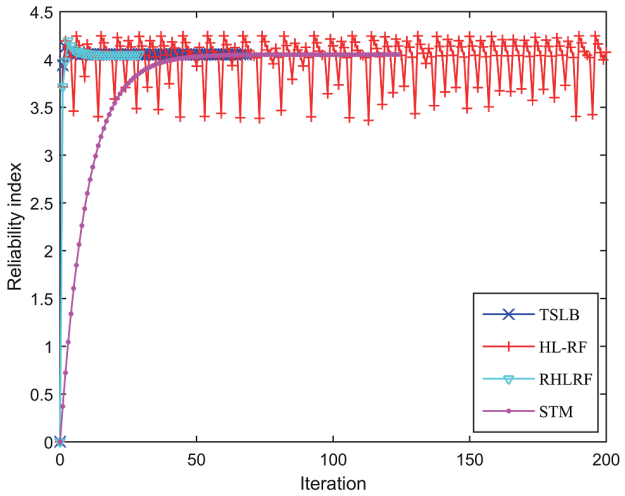

Fig. 16 Iteration history in example 5

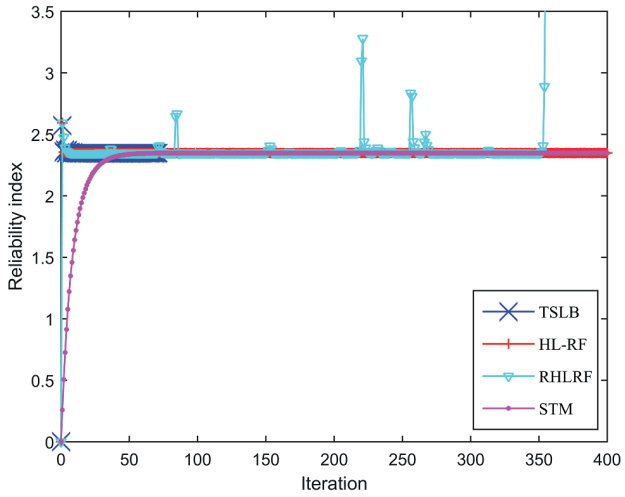

Fig. 17 Iteration history in example 6

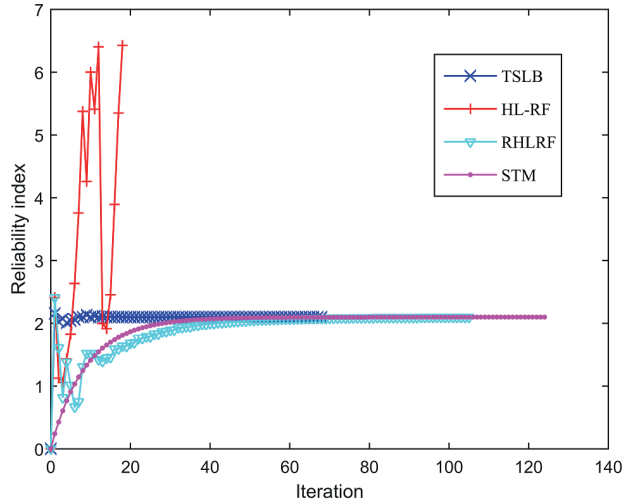

Fig. 18 Iteration history in example 7

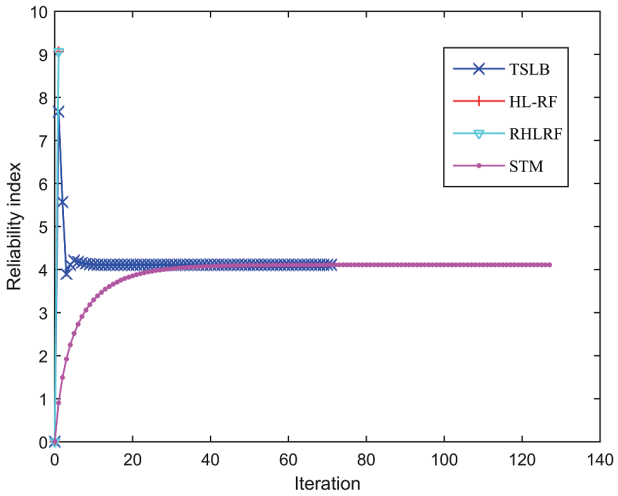

Fig. 19 Iteration history in example 8

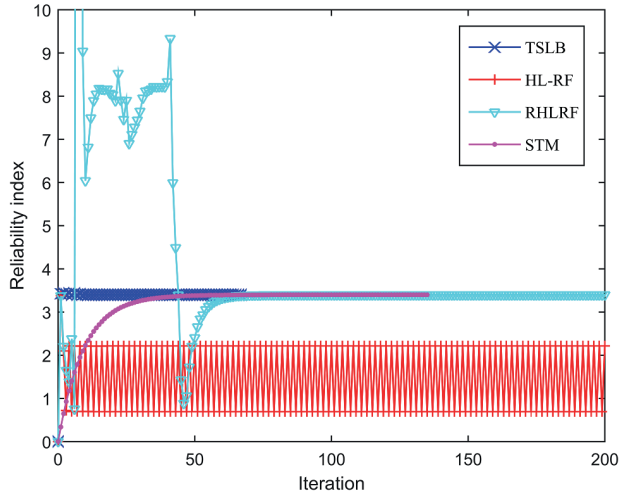

Fig. 20 Iteration history in example 9

are gathered in Table 5. According to Figs. 12–20 or Table 5, in all problems, HL-RF shows instability and fails to stabilize and converge. In examples 1 and 2, whose difference is only in a mixed term, a slight oscillation prevents HL-RF from convergence. In example 3, the periodic behavior of HL-RF can be observed more clearly. The slight oscillation of HL-RF can be seen in example 4, too. The general form of the diagrams for examples 1–4 (Figs. 12–15) are similar but the final values are different, as reported in Table 5. In these four examples, three other methods are successful in convergence with TSLB taking the least iterations. Besides, in these examples, RHL-RF requires fewer iterations than STM except in example 3.

After considering the polynomials of examples 1–4, in example 5, a cosine function is added to a polynomial to increase the nonlinearity. As seen in Fig. 16, HL-RF cannot deal with this nonlinearity and behaves chaotically. Such behaviors have been investigated by Yang et al. [20]. Fig. 21 is presented to show the reason. As it can be observed in the figure, in some cases the gradient vector at U1 takes the design point of the current

Table 5 Comparison of the results in numerical examples

Example	TSLB			HLRF		RHLRF			STM			Literature
	β	Iter.	time (sec)	β	Iter.	β	Iter.	time (sec)	β	Iter.	time (sec)	
1	2.2260	63	0.0262	NC		2.2260	111	0.0414	2.2260	141	0.0333	–β = 2.2260 [31] –β = 2.2259 [19] –β = 2.2260 [24] –β = 2.5328 (MCS) –β = 2.6163 (SORM)
2	2.2983	63	0.0298	NC		2.2982	124	0.0470	2.2982	144	0.0350	–β = 2.2983 [18] –β = 2.2983 [24] –β = 2.2982 [32] –β = 2.2983 [25] –β = 2.5274 (MCS) –β = 2.6259 (SORM)
3	2.3655	61	0.0280	NC		2.3654	195	0.0522	2.3654	163	0.0344	–β = 2.3633 [18] –β = 2.3628 [24] –β = 2.3655 [33] –β = 2.3655 [25] –β = 2.9019 (MCS) –β = 2.8450 (SORM)
4	1.9003	65	0.0411	NC		1.9003	74	0.0701	1.9003	132	0.0585	–β = 1.9002 [19] –β = 1.9003 [34] –β = 2.2296 (MCS) –β = 2.2372 (SORM)
5	4.0519	68	0.0581	NC		4.0519	29	0.0621	4.0519	124	0.0615	–β = 4.275 [35] –β = 4.12 [24] –β = 3.7190 (MCS) –β = 4.2244 (SORM)
6	2.3482	71	0.0702	NC			NC			NC		–β = 2.3482 [17] –β = 2.3483 [31] –β = 2.3483 [24] –β = 2.2523 (MCS) –β = 2.2625 (SORM)
7	2.0982	68	0.0733	NC		2.0966	105	0.1940	2.0981	124	0.0892	–β = 2.12 [36] –β = 2.0163 [32] –β = 2.1231 [25] –β = 2.1373 [30] –β = 2.7360 (MCS) –β = 2.6706 (SORM)
8	4.1108	71	0.0712	NC			NC			127		0.0890	–β = 4.1165 [30] –β = 4.0253 (MCS) –β = 4.0932 (SORM)
9	3.3997	67	0.0741	NC			NC			135		0.0973	–β = 3.3753 [30] –β = 3.7852 (MCS) –β = 3.8316 (SORM)

NC: Not Converged

iteration to U2. Then the gradient vector at U2 takes it back to U1 (or close to it). This is the reason HLRF falls in such traps and expresses unstable behaviors. Employing smaller step sizes or changing step sizes in iterations are the possible choices for this problem. Among three other methods converging in this problem, RHL-RF need the least iterations and STM needs the most. TSLB stands at the middle in this problem. Example 6 represents a sensitive LSF including noise terms. This function is usually employed in reliability literature to test the strength of new proposed methods. Fig. 17 shows the iteration history of the investigated methods. As one can observe, the noise of the LSF is such disruptive that all methods except TSLB fail to converge. HL-RF and STM do not get

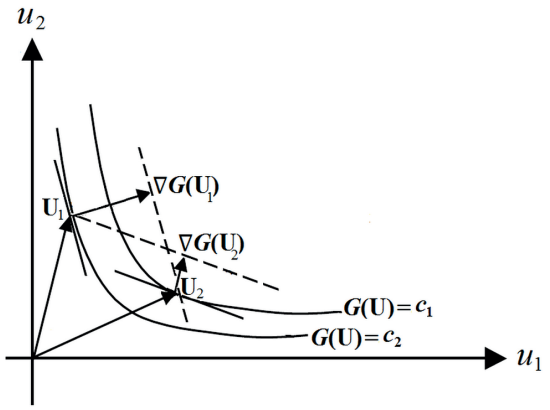

Fig. 21 Periodic or chaotic solution for design point in iterations [20]

stable around the answer in 400 iterations and RHL-RF goes infinitely high after iteration 350. However, even in such a nonlinear case, TSLB stably finds the answer after 71 iterations. This can be a sign for the robustness of the proposed method. Spring system of example 7 is another nonlinear case in which HL-RF fails very soon before iteration 20, as depicted in Fig. 18. According to this figure, TSLB and STM converge with the least and most iterations, respectively. The LSF of Eq. (29), associated with the structural element of example 8, is a highly nonlinear case, too. The nonlinearity of this problem is so extreme that HL-RF and RHL-RF diverge simultaneously before the second iteration (Fig. 19). However, TSLB and STM express robustness in this example. Besides, the required iterations for convergence in TSLB are fewer than that in STM. In example 9, a cantilever tube is investigated. The highly nonlinear LSF of this tube causes HL-RF to behave improperly. The periodic behavior of HL-RF can be observed in Fig. 20. Due to the extreme nonlinearity of the LSF, RHL-RF encounters chaotic behavior in the initial iterations and then oscillates around the answer without getting stable in 200 iterations. Like example 8, TSLB and STM are the successful methods and TSLB finishes the job using fewer iterations.

The values of Figs. 12–20 are represented in Table 5 for convenience. Based on this table, or the represented figures and aforementioned explanations, HL-RF diverges in all 9 examples, RHL-RF diverges in 3 examples (6, 8 and 9) and STM diverges in example 6. In contrast, TSLB is the only method, which could converge in all represented numerical examples, without any failure and divergence. In fact, the diagrams clearly show that TSLB finally finds a way for convergence in all nonlinear examples, without any sign of periodic or chaotic behaviors. The stability of the proposed algorithm in the represented highly nonlinear mathematical and structural problems indicates the robustness of the algorithm. This stability in the proposed algorithm can be associated with the second step of each iteration, in which $\boldsymbol{U}'_k$ is pushed such that it approaches limit state surface. By this movement, the next iteration can start from a point closer to limit state surface. In fact, starting each iteration from the neighborhood of limit state surface helps to stabilize the process, especially in highly nonlinear cases where large distances from limit state surface may result in divergence. It is noteworthy that examples like examples 6, 8 and 9 are of those examples usually employed to test the robustness of the proposed methods of the literature. For instance, example 6 without the sinuous terms and their relatively small multiplier can be solved by many methods. However, adding six sinuous terms multiplied by 0.001 creates a new challenge and generates instability, and therefore the problem becomes so sensitive to small movements. Many methods fail in encountering this challenge and show numerical instability. In Table 5, it is observed that even STM, which benefits from the chaos control concept, fails in this robustness test. That is why this example is a very suitable and common example for testing the methods focusing on robustness. Examples 8 and 9 are two other examples of the literature, designed to test the robustness of the new represented methods. The ability of the proposed method in dealing with such examples is a sign for the robustness of the proposed method. As previously mentioned, this ability can be associated with: (1) separating the goals, generally followed in a reliability method (i.e., separating Eqs. (8) and (9) as two distinct goals), and (2) assigning a specific and separate tool to reach each goal ($\alpha_k \boldsymbol{d}_k$ is the first tool and $\gamma_k \boldsymbol{S}_k$ is the second tool to make Eqs. (8) and (9) satisfied). Since each single step concentrates on one goal, it pushes to that goal more properly. This can be considered an example of novelty of the proposed algorithm.

There is also another item providing a powerful tool for the robustness of the proposed method. This item is the potential of adjustable step size α_k. The fact that α_k can be adjusted (automatically like what proposed herein or by the user) gives a great possibility to the method to be able to deal with extremely nonlinear cases. Reliability function works here as a useful criterion. Actually, when nonlinearity is relatively high, it shows itself in f_k increasing compared to f_{k-1}. When this signal is sent in an iteration, α_k is immediately reduced to adapt with the high existing nonlinearity and to keep the robustness. If the signal of $f_k > f_{k-1}$ is not sent, the computation process continues

without any change in α_k. Generally, the combination of the limit state function and reliability function (based on the above-mentioned separation of goals), alongside the effective application of a control parameter (α_k) and a non-linearity criterion (reliability function in two successive iterations) are the novelties of the current paper.

Comparing the reliability index of the proposed algorithm with that of other methods of Table 5 (especially STM which is considered an accurate method), one can conclude that the proposed algorithm is accurate, too. It should be noted that this accuracy is obtained using a reasonable number of iterations. As observed in the columns of "iterations" of Table 5, the proposed algorithm is sufficiently efficient and therefore can be employed in numerical problems.

Apart from four aforementioned methods, the answers existing in the literature are summarized in the last column of Table 5 as reference values. Besides, the results of MCS and second-order reliability method (SORM) are included at the end of this column. In MCS, 10^6 samples are generated, except examples 5, 8 and 9 in which 2×10^6 samples are generated due to lower probability of failure or higher reliability index. For SORM, Breitung's formula have been applied. What should be mentioned about the table is that the relative difference with MCS or SORM is not due to the error in finding the location of design point, and it is actually the matter of different definitions. In fact, four investigated methods try to find the minimum distance of LSF from the origin of U-space, in the geometric sense. Other methods of the literature (as FORM) have reported the same values for reliability index (as seen in the last column), because they have the same target and this target has been defined to specify the location of design point. However, the target in MCS is to find the distribution of LSF and to compute probability of failure. Then reliability index is just reported using the popular relation of FORM, $\beta = -\Phi^{-1}(P_f)$. Or in SORM the curvatures of the LSF at design point has been taken into account for better estimation of probability of failure, and reliability index is reported by the above-mentioned relation of FORM. This β may be different in some nonlinear cases from the common geometric reliability index defined by Hasofer and Lind [15]. Thus, in such cases, it may be better to compare the reliability index of the methods of FORM with each other to evaluate their accuracy in finding the location of design point. SORM is a powerful tool to improve the estimation of probability of failure based on the value of reliability index, the location of design point, and the curvatures of LSF at design point.

Another point in Table 5 is that the proposed algorithm shows a good performance in the examples including random variables with high coefficient of variation (δ). In examples 1–4 and 7 there are variables with $\delta = 0.5$ which is considered a large value. According to Table 5, even in such examples the proposed algorithm can work properly in keeping convergence [17–19, 24, 25, 30–36].

It is noteworthy that the proposed algorithm, as an approximation gradient-based method, requires the explicit form of limit state function and its derivatives for the gradient vector. While in many problems, the function cannot be explicitly expressed, or it is not differentiable. To circumvent this limitation of the proposed algorithm, numerical methods for evaluation of the gradient vector should be applied (e.g., finite difference method). However, such numerical methods may impose larger computational burden compared to the non-gradient-based methods. There is also another limitation associated with the proposed algorithm. As it was mentioned before, the adjustable step size α_k is a control tool for robustness, i.e., if convergence is not achieved by an initial assumption of α_k, it can be reduced. By this reduction of step size, the convergence can be achieved. However, it is not clear from the beginning whether there was another initial value of α_k which could achieve convergence faster, and therefore it is up to the user's choice for initial α_k.

One point about the proposed algorithm is that it has strongly focused on the robustness. The efficiency of the proposed algorithm can be increased by manipulating the control parameter α_k in several ways. For instance, Barzilai-Borwein gradient method is an efficient numerical method using line search in iterations. The same approach can be implemented on α_k in each iteration to reach better values. In fact, line search could be one possible approach to speed up the rate of convergence, provided that a suitable criterion could be found through an investigation to be applied within iterations.

To sum up briefly, the algorithm of the present paper is robust and relatively efficient, as it is clear from the results of numerical examples. Due to its robustness, it can be trusted in applications. Thus, the proposed algorithm can be a possible choice to be used in practical cases.

5 Conclusions

This paper proposes an iterative algorithm for structural reliability analysis. The proposed algorithm benefits from the contribution of Lagrange function in its formulation. In each iteration, the purpose of minimizing the Lagrange function

is followed by moving in a descent direction. Besides, for satisfying the existing constraint and for a better search of design point, each iteration starts from the vicinity of limit state surface. The performance of the whole procedure has been shown in nonlinear mathematical and structural problems. While HL-RF is not sufficiently robust and simulation methods are time-consuming and inefficient, the proposed algorithm benefiting from reliability function and limit state function simultaneously, can be used as a possible alternative in structural reliability analysis.

Acknowledgments
This research did not receive any specific grant from funding agencies in the public, commercial, or not-for-profit sectors.

References

[1] Zaeimi, M., Ghoddosain, A. "System Reliability Based Design Optimization of Truss Structures with Interval Variables", Periodica Polytechnica Civil Engineering, 64(1), pp. 42–59, 2020. https://doi.org/10.3311/PPci.14238

[2] Ding, F., Xiong, S., Zhang, H., Li, G., Zhao, P., Xiang, P. "Reliability analysis of axial bearing capacity of concrete filled steel tubular stub columns with different cross sections", Structures, 33, pp. 4193–4202, 2021. https://doi.org/10.1016/j.istruc.2021.04.006

[3] Asghshahr, M. S. "Reliability Based Design Optimization of Reinforced Concrete Frames Using Genetic Algorithm", Periodica Polytechnica Civil Engineering, 65(2), pp. 566–576, 2021. https://doi.org/10.3311/PPci.17150

[4] Shayanfar, M. A., Barkhordari, M. A., Roudak, M. A. "An adaptive importance sampling-based algorithm using the first-order method for structural reliability", International Journal of Optimization in Civil Engineering, 7(1), pp. 93–107, 2017. [online] Available at: http://ijoce.iust.ac.ir/article-1-286-en.html

[5] Shayanfar, M. A., Barkhordari, M. A., Roudak, M. A. "A new effective approach for computation of reliability index in nonlinear problems of reliability analysis", Communications in Nonlinear Science and Numerical Simulation, 60, pp. 184–202, 2018. https://doi.org/10.1016/j.cnsns.2018.01.016

[6] Kaveh, A., Biabani Hamedani, K., Kamalinejad, M. "Set Theoretical Variants of Optimization Algorithms for System Reliability-based Design of Truss Structures", Periodica Polytechnica Civil Engineering, 65(3), pp. 717–729, 2021. https://doi.org/10.3311/PPci.17519

[7] Xiao, N.-C., Zuo, M. J., Guo, W. "Efficient reliability analysis based on adaptive sequential sampling design and cross-validation", Applied Mathematical Modelling, 58, pp. 404–420, 2018. https://doi.org/10.1016/j.apm.2018.02.012

[8] Seger, M. A., Kisgyörgy, L. "Estimation of Link Choice Probabilities Using Monte Carlo Simulation and Maximum Likelihood Estimation Method", Periodica Polytechnica Civil Engineering, 64(1), pp. 20–32, 2020. https://doi.org/10.3311/PPci.14366

[9] Liu, X., Zheng, S., Wu, X., Chen, D., He, J. "Research on a seismic connectivity reliability model of power systems based on the quasi-Monte Carlo method", Reliability Engineering & System Safety, 215, 107888, 2021. https://doi.org/10.1016/j.ress.2021.107888

[10] Roudak, M. A., Shayanfar, M. A., Karamloo, M. "Improvement in first-order reliability method using an adaptive chaos control factor", Structures, 16, pp. 150–156, 2018. https://doi.org/10.1016/j.istruc.2018.09.010

[11] Zhang, X., Wu, Z., Ma, H., Pandey, M. D. "An effective Kriging-based approximation for structural reliability analysis with random and interval variables", Structural and Multidisciplinary Optimization, 63, pp. 2473–2491, 2021. https://doi.org/10.1007/s00158-020-02825-8

[12] Kaveh, A., Hoseini Vaez, S. R., Hosseini, P., Fathali, M. A. "Heuristic Operator for Reliability Assessment of Frame Structures", Periodica Polytechnica Civil Engineering, 65(3), pp. 702–716, 2021. https://doi.org/10.3311/PPci.17580

[13] Bucher, C. G. "Adaptive sampling — an iterative fast Monte Carlo procedure", Structural Safety, 5(2), pp. 119–126, 1988. https://doi.org/10.1016/0167-4730(88)90020-3

[14] Cornell, C. A. "A probability based structural code", Journal Proceedings, 66(12), pp. 974–985, 1969.

[15] Hasofer, A. M., Lind, N. C. "Exact and invariant second-moment code format", Journal of the Engineering Mechanics Division, 100(1), pp. 111–121, 1974. https://doi.org/10.1061/JMCEA3.0001848

[16] Rackwitz, R., Flessler, B. "Structural reliability under combined random load sequences", Computers & Structures, 9(5), pp. 489–494, 1978. https://doi.org/10.1016/0045-7949(78)90046-9

[17] Liu, P.-L., Der Kiureghian, A. "Optimization algorithms for structural reliability", Structural Safety, 9(3), pp. 161–177, 1991. https://doi.org/10.1016/0167-4730(91)90041-7

[18] Wang, L., Grandhi, R. V. "Safety index calculation using intervening variables for structural reliability analysis", Computers & Structures, 59(6), pp. 1139–1148, 1996. https://doi.org/10.1016/0045-7949(96)00291-X

[19] Santosh, T. V., Saraf, R. K., Ghosh, A. K., Kushwaha, H. S. "Optimum step length selection rule in modified HL–RF method for structural reliability", International Journal of Pressure Vessels and Piping, 83(10), pp. 742–748, 2006. https://doi.org/10.1016/j.ijpvp.2006.07.004

[20] Yang, D., Li, G., Cheng, G. "Convergence analysis of first order reliability method using chaos theory", Computers & Structures, 84(8–9), pp. 563–571, 2006. https://doi.org/10.1016/j.compstruc.2005.11.009

[21] Yang, D. "Chaos control for numerical instability of first order reliability method", Communications in Nonlinear Science and Numerical Simulation, 15(10), pp. 3131–3141, 2010. https://doi.org/10.1016/j.cnsns.2009.10.018

[22] Gong, J.-X., Yi, P. "A robust iterative algorithm for structural reliability analysis", Structural and Multidisciplinary Optimization, 43, pp. 519–527, 2011. https://doi.org/10.1007/s00158-010-0582-y

[23] Keshtegar, B., Miri, M. "An enhanced HL-RF method for the computation of structural failure probability based on relaxed approach", Civil Engineering Infrastructures Journal, 46(1), pp. 69–80, 2013. https://doi.org/10.7508/CEIJ.2013.01.005

[24] Gong, J., Yi, P., Zhao, N. "Non-Gradient–Based Algorithm for Structural Reliability Analysis", Journal of Engineering Mechanics, 140(6), 04014029, 2014. https://doi.org/10.1061/(asce)em.1943-7889.0000722

[25] Roudak, M. A., Shayanfar, M. A., Barkhordari, M. A., Karamloo, M. "A robust approximation method for nonlinear cases of structural reliability analysis", International Journal of Mechanical Sciences, 133, pp. 11–20, 2017. https://doi.org/10.1016/j.ijmecsci.2017.08.038

[26] Roudak, M. A., Shayanfar, M. A., Barkhordari, M. A., Karamloo, M. "A new three-phase algorithm for computation of reliability index and its application in structural mechanics", Mechanics Research Communications, 85, pp. 53–60, 2017. https://doi.org/10.1016/j.mechrescom.2017.08.008

[27] Shayanfar, M. A., Barkhordari, M. A., Roudak, M. A. "An efficient reliability algorithm for locating design point using the combination of importance sampling concepts and response surface method", Communications in Nonlinear Science and Numerical Simulation, 47, pp. 223–237, 2017. https://doi.org/10.1016/j.cnsns.2016.11.021

[28] Shayanfar, M. A., Barkhordari, M. A., Roudak, Mohammad A. "Locating design point in structural reliability analysis by introduction of a control parameter and moving limited regions", International Journal of Mechanical Sciences, 126, pp. 196–202, 2017. https://doi.org/10.1016/j.ijmecsci.2017.04.003

[29] Shayanfar, M. A., Barkhordari, M. A., Roudak, M. A. "A Modification to HL-RF Method for Computation of Structural Reliability Index in Problems with Skew-distributed Variables", KSCE Journal of Civil Engineering, 22(8), pp. 2899–2905, 2018. https://doi.org/10.1007/s12205-017-1473-1

[30] Roudak, M. A., Karamloo, M. "Establishment of non-negative constraint method as a robust and efficient first-order reliability method", Applied Mathematical Modelling, 68, pp. 281–305, 2019. https://doi.org/10.1016/j.apm.2018.11.021

[31] Wang, L., Grandhi, R. V. "Efficient safety index calculation for structural reliability analysis", Computers & Structures, 52(1), pp. 103–111, 1994. https://doi.org/10.1016/0045-7949(94)90260-7

[32] Keshtegar, B. "Chaotic conjugate stability transformation method for structural reliability analysis", Computer Methods in Applied Mechanics and Engineering, 310, pp. 866–885, 2016. https://doi.org/10.1016/j.cma.2016.07.046

[33] Periçaro, G. A., Santos, S. R., Ribeiro, A. A., Matioli, L. C. "HLRF–BFGS optimization algorithm for structural reliability", Applied Mathematical Modelling, 39(7), pp. 2025–2035, 2015. https://doi.org/10.1016/j.apm.2014.10.024

[34] Santos, S. R., Matioli, L. C., Beck, A. T. "New Optimization Algorithms for Structural Reliability Analysis", Computer Modeling in Engineering & Sciences, 83(1), pp. 23–56, 2012. https://doi.org/10.3970/cmes.2012.083.023

[35] Gavin, H. P., Yau, S. C. "High-order limit state functions in the response surface method for structural reliability analysis", Structural Safety, 30(2), pp. 162–179, 2008. https://doi.org/10.1016/j.strusafe.2006.10.003

[36] Der Kiureghian, A., De Stefano, M. "Efficient algorithm for second-order reliability analysis", Journal of Engineering Mechanics, 117(12), pp. 2904–2923, 1991. https://doi.org/10.1061/(ASCE)0733-9399(1991)117:12(2904)